

# Geophysical Research Letters®



## RESEARCH LETTER

10.1029/2024GL108732

## To Rotate or to Link? The Connection Between the Red Sea and Gulf of Aden Rifts in Central Afar

Ameha Muluneh<sup>1,2,3</sup> , Sascha Brune<sup>2,4</sup> , Carolina Pagli<sup>5</sup> , Alessandro La Rosa<sup>5</sup> ,  
Derek Keir<sup>6,7</sup> , Derek Neuharth<sup>8</sup>, and Giacomo Corti<sup>9</sup> 

<sup>1</sup>Addis Ababa University, Addis Ababa, Ethiopia, <sup>2</sup>GFZ German Research Centre for Geosciences, Potsdam, Germany, <sup>3</sup>Center for Marine Environmental Sciences, University of Bremen, Bremen, Germany, <sup>4</sup>University of Potsdam, Potsdam, Germany, <sup>5</sup>University of Pisa, Pisa, Italy, <sup>6</sup>University of Florence, Florence, Italy, <sup>7</sup>University of Southampton, Southampton, UK, <sup>8</sup>ETH Zurich, Zürich, Switzerland, <sup>9</sup>CNR National Research Council of Italy, Florence, Italy

### Key Points:

- Analyzing the spatiotemporal evolution of rifts can address the controversial issue on the connection between propagating rifts
- We present results from InSAR and geodynamic models to describe the connection between Red Sea (RS) and Gulf of Aden (GoA) rifts in central Afar
- The connection between the two rifts evolves from rift overlap to direct linkage elucidating the observed deformation in the region

### Supporting Information:

Supporting Information may be found in the online version of this article.

### Correspondence to:

A. Muluneh,  
[ameha@gfz-potsdam.de](mailto:ameha@gfz-potsdam.de)

### Citation:

Muluneh, A., Brune, S., Pagli, C., La Rosa, A., Keir, D., Neuharth, D., & Corti, G. (2024). To rotate or to link? The connection between the red sea and Gulf of Aden rifts in central afar. *Geophysical Research Letters*, *51*, e2024GL108732. <https://doi.org/10.1029/2024GL108732>

Received 6 FEB 2024

Accepted 5 JUN 2024

**Abstract** Central Afar is shaped by the interaction between the Red Sea (RS) and Gulf of Aden (GoA) rifts. While there have been several studies conducted in the region, we know surprisingly little about the mechanism of connection between these two rift branches. Here we use high-resolution 3D lithospheric scale geodynamic modeling to capture the evolution of linkage between the RS and GoA rifts in central Afar. Our results demonstrate that the two rifts initially overlap and interact across a broad zone of faulting and vertical axis block rotation. However, through time, rift overlap is abandoned in favor of direct linkage which generates a series of localized en-echelon basins. The present-day direct linkage between the two rifts is supported by geodetic observations. Our study reconciles previously proposed models for the RS and GoA rift connection by considering spatial and temporal evolution of the rifts.

**Plain Language Summary** Rifts are places where tectonic plates move away from each other. They normally start as short, isolated features, and then grow and connect together to eventually form oceans. Central Afar in East Africa is a great location to study how these rifts form and grow by connecting with other rifts. In this area, the Red Sea (RS) and Gulf of Aden (GoA) rifts interact, but it is not clear how this happened through time. Some studies suggest that the two rifts form an overlap zone where blocks within the overlap rotate, while others argue that the two rifts directly link and form a continuous rift zone. To resolve this debate, we conducted a high-resolution computer simulation of the evolution of the RS and GoA rifts in central Afar. We compared our model results with earthquake positions and satellite data that constrain the present-day motion of the plates. Our results demonstrate that the RS and GoA rifts first overlapped for a few millions of years, and then formed a direct linkage. Our study suggests that both conceptual models can be reconciled when we consider the temporal evolution of the two rifts through geological times.

## 1. Introduction

The interaction and linkage between two propagating rift segments during continental breakup play a major role in shaping continental rifted margins. Important insights regarding rift linkage are gained from observations (Ebinger et al., 2000; Kolawole et al., 2021; La Rosa et al., 2022; Nelson et al., 1992), and modeling experiments (Balázs et al., 2023; Brune et al., 2017; Le Pourhiet et al., 2017; Wolf et al., 2022; Zwaan & Schreurs, 2017). According to these studies, two rifts link either via a transform fault, a single curved ridge, rift tip splay (tip bifurcation), or they form an overlap zone. However, in most rifts globally it is unclear which mechanism is responsible for rift linkage, what the controlling factors are, and how the mechanism changes in space and time (e.g., Allken et al., 2012; Neuharth et al., 2021).

The Afar rift, East Africa, is one of the few places in the world where we can directly observe tectonic processes related to rift interaction and linkage during the late stage of continental rifting (e.g., Rime et al., 2023). Here, the linkage between active segments occurs at a range of scales and stages of rift evolution. For example, Illsley-Kemp et al. (2018) and La Rosa et al. (2022) showed that the linkage between closely spaced, en-echelon segments in the northern Afar (Figure 1a), where the rift is close to breakup, occurs via localized oblique slip on a conjugate fault set. On the contrary, the central Afar rift system is broad and less evolved and characterized by a wide and complex network of distributed faults (Doubré et al., 2017; Pagli et al., 2014). The distributed deformation is generally attributed to central Afar being a zone of linkage between highly localized extension at both

© 2024. The Author(s).

This is an open access article under the terms of the [Creative Commons Attribution License](https://creativecommons.org/licenses/by/4.0/), which permits use, distribution and reproduction in any medium, provided the original work is properly cited.

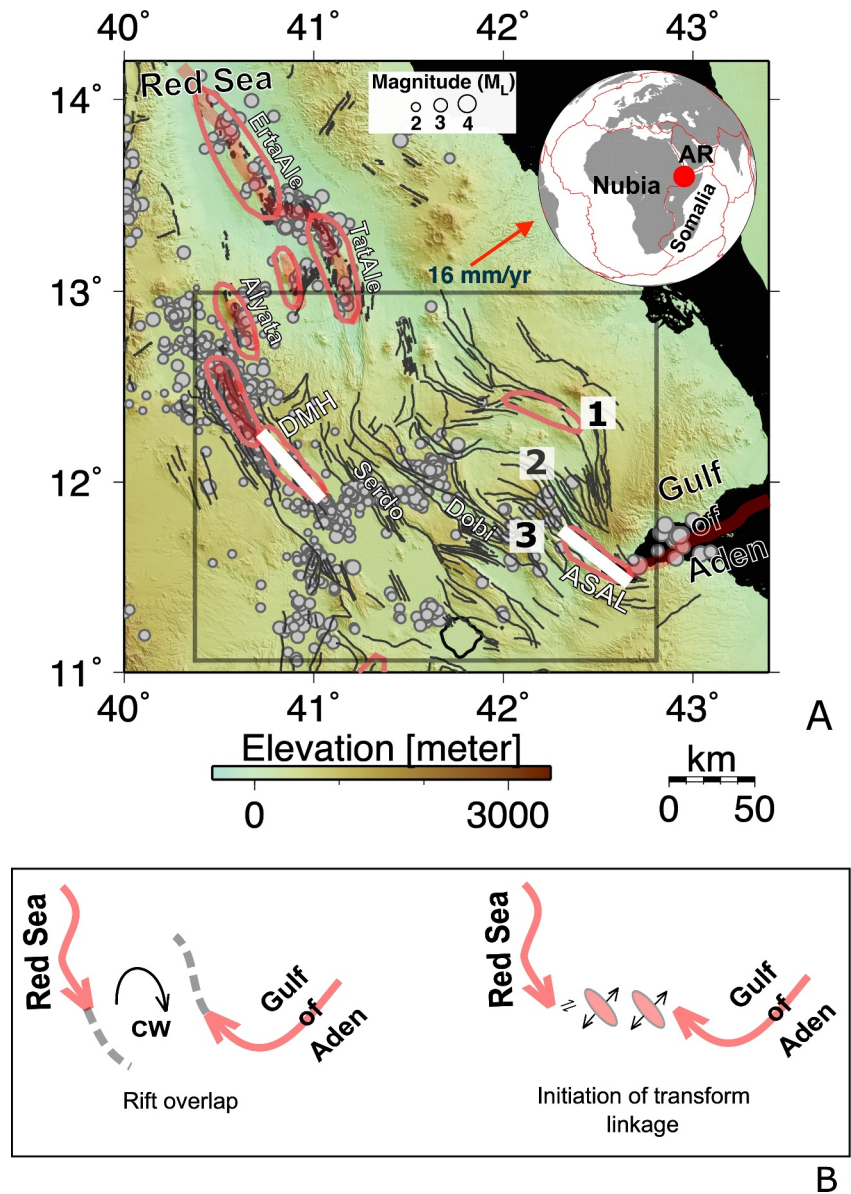


**Figure 1.** (a) Location of central Afar. The gray circles are earthquake epicenters (Pagli et al., 2018). AR—Arabia. The thick white lines at the Dabbahu-Manda Harraro (DMH) and ASAL segments indicate the orientation and portion of the Red Sea (RS) and Gulf of Aden (GoA) rifts modeled here (Figure 3a). The red ovals indicate the active rift segments in the region (Wolfenden et al., 2004). The numbers 1, 2, 3, show progressive strain localization from block bounding faults (1) to curved faults at their tips (2) to NW-SE oriented faults in the Dobi basin (3) attested by distribution of faults in central afar (Manighetti et al., 1998). The Dobi and Serdo grabens are considered as the locus of deformation between the DMH and ASAL segments (b) Proposed models for the connection between the RS and GoA rifts. The open gray box in (a) bounds the study area shown in Figure 2. The red arrow in (a) shows the general opening of central Afar rift. CW = clockwise rotation.

the Dabbahu-Manda Harraro (DMH) segment of the southern Red Sea (RS) rift, and the Asal-Ghobbet (hereafter called ASAL) segment of the western Gulf of Aden (GoA) rift (Figure 1a; Moore et al., 2021).

Since ~3 Ma, extension in central Afar is thought to have become localized to the 60-km-long, 10-km-wide DMH and ASAL segments (Figure 1; Wright et al., 2006; Almalki & Betts, 2021). These two segments are left stepping, and offset from each other by ~100 km in a right-lateral sense. However, the mechanism of linkage between the two segments has been a long-standing topic of debate that can be summarized in terms of two conceptual models (Figure 1b). On one hand, the pattern of faulting coupled with paleomagnetic observations from mostly ~1–2 Ma

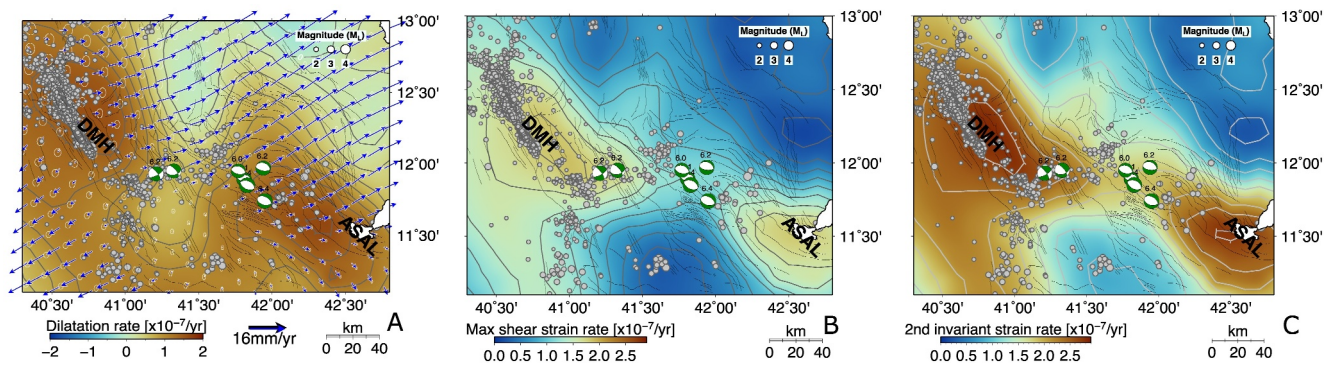


**Figure 2.** Deformation maps, a to c, indicate dilatation (positive values are extension), maximum shear strain, and second invariant strain rates, respectively, derived from horizontal velocity field (arrows in a). The gray lines are contours of respective fields. The earthquake focal mechanisms (green—extension and white—compression) are taken from Craig et al. (2011). The numbers show the local magnitude of the focal mechanisms.

Stratoid basalts has been put forward to show that the RS and GoA rifts substantially overlap causing blocks within the overlapping region to rotate in a clockwise sense (Acton et al., 1991; Kidane et al., 2003; Muluneh et al., 2013). On the other hand, geodetic data and strain rate analysis from the last ~20 years suggest that the RS and GoA do not substantially overlap and that linkage between the two rifts occurs through a belt of overlapping, left-stepping series of extensional basins, with dextral shear occurring at the lateral edges of the linkage zone (Demissie et al., 2023; Pagli et al., 2018; Polun et al., 2018).

The discrepancy between these models could be accounted for by the difference in timescale of observations and that each method constrains different stages of rift evolution. Geodetic methods constrain decadal deformations and may not provide insight into the long-term propagation and linkage of rifts over geologic time scales, that is, millions of years. We present lithospheric scale 3D numerical experiments using ASPECT (Advanced Solver for Planetary Evolution, Convection, and Tectonics; Gassmöller et al., 2018; Glerum et al., 2018, 2020; Heister et al., 2017; Kronbichler et al., 2012; Rose et al., 2017) to constrain the evolution of strain accommodation mechanisms in central Afar. Our model results, in conjunction with high-resolution geodetic data interpretation and geological/paleomagnetic data, captured the stages of deformation from overlap to direct linkage suggesting that both rift connection models can be reconciled when considering space and time evolution of rifts.

## 2. Deformation Rate From Geodesy

The present-day deformation of the Afar rift is well constrained by geodetic observations (Moore et al., 2021; Pagli et al., 2014). Here we combine available GPS data (Dobre et al., 2017) with InSAR from two different Sentinel-1a/b tracks in ascending and descending geometries spanning the period between 2014 and 2021 to generate a high-resolution continuous 3D velocity field for central Afar following the method described in Pagli et al. (2014). Then we calculate the horizontal strain rates (Cardozo & Allmendinger, 2009; M. Wang & Shen, 2020) (See the Supporting Information S1 file for strain rate analysis). Our results show that the highest extensional and shear strain rates occur at the DMH and ASAL segments (Figure 2), likely due to the presence of crustal magma (Drouin et al., 2017). Outside of the two magmatic segments, relatively higher strain rates occur in a ~ NW-SE oriented region between the DMH and ASAL segments and at the southern tip of the DMH segment. While the strain localization at the southern tip of the DMH could be related to the formation of the triple junction in central Afar (Maestrelli et al., 2022), the higher strain rate between the DMH and ASAL segments clearly indicates incipient linkage between them.

Combining the strain rate analysis with the pattern of local seismicity (Pagli et al., 2018) and the faulting style inferred from teleseismic earthquake focal mechanisms (Craig et al., 2011) in the Dobi basin (Figure 1a), we hypothesize that the linkage between the DMH and ASAL segments currently occurs via a series of en-echelon basins of dominantly normal dip slip, within an overall transtensional zone bound by oblique and strike slip faults (Pagli et al., 2018).



### 3. Geodynamic Model Setup

The DMH and ASAL segments belonging to the RS and GoA rifts, respectively, form two nearly parallel, en echelon, left-steeping segments in central Afar (Figure 1a). We setup a numerical modeling experiment using the ASPECT software to capture spatial and temporal evolution of the deformation pattern during the connection between these two segments. We construct a 3D lithospheric scale box model setup (Figure 2a) with dimensions of  $400 \times 400 \times 100$  km in  $X$ ,  $Y$ , and  $Z$  directions, respectively. We use the adaptive mesh refinement capability of ASPECT to model the region where rift linkage occurs with a maximum resolution of 2.5 km (in the area marked by gray box in Figure 3a). Far-field motion is imposed by specifying velocities on both the left and right model boundaries. We applied a constant total extension rate of 16 mm/yr (Vigny et al., 2007). Plate reconstructions and geological studies show no evidence for a significant change in plate motions relevant for our study area for at least the last 10–15 Myrs (e.g., McClusky et al., 2010). In all model runs, we use an initial 30 km thick crust dominated by wet anorthite rheology (Rybacki et al., 2006), which is chosen based on high  $V_p/V_s$  ratio ( $>1.8$ ) in central Afar (Ahmed et al., 2022; Hammond et al., 2011; T. Wang et al., 2021). In doing so we assume that crustal composition has not changed dramatically during the last few million years, which is justified given the magmatism that has affected Afar over tens of millions of years. The lithospheric mantle and asthenosphere are modeled by dry and wet olivine rheology, respectively (Hirth & Kohlstedt, 2003) (Table S1; see the Supporting Information S1).

The model's depth to the lithosphere-asthenosphere boundary (LAB) is based on multiple data sets. Tomographic images suggest that the LAB depth occurs at  $\sim 75$  km (Bastow et al., 2008; Chambers et al., 2022). Similarly, receiver functions derived from joint inversion of surface and body waves show that the LAB beneath the western flank of the Afar rift occurs at depth ranges of 60–80 km (Dugda et al., 2005). This is consistent with S-P receiver function studies which image a weak LAB beneath Afar at  $\sim 70$  km depth (Lavayssiere et al., 2018). The range of depths for the LAB suggested by seismic imaging is broadly consistent with petrological modeling which suggest the top of the Afar melt zone, and by implication the LAB, is at  $\sim 65$ –85 km depth (Ferguson et al., 2013; Watts et al., 2023). Figures 3b–3e shows the reference model for the evolution of linkage between the DMH and ASAL segments. As the tectonic regime during rift linkage is highly influenced by the thickness of the lithosphere, we test its impact by varying the thickness of the lithospheric mantle while keeping the crustal thickness fixed at 30 km.

The linkage regime is also controlled by the rift-perpendicular offset (i.e., in  $x$ -direction) between rift segments (Neuharth et al., 2021). To assess its impact, we run a suite of models assuming different lithospheric thicknesses and  $x$ -offsets. Figure 4 shows a regime diagram for lithospheric thicknesses of 60, 70, and 80 km (i.e., 30, 40, and 50 km thick lithospheric mantle with a 30 km thick crust) and  $x$ -offsets of 50, 100, and 150 km, while the  $y$ -offset is held fixed at 50 km. We calculate the strain rate at each time step in order to compare our model simulations to strain rate maps derived from combinations of InSAR and GPS. The models have been running for 5 million years since their initiation, as shown in Figure 3. Strain localization has affected central Afar since  $\sim 4$ –3 Ma. Therefore, Figure 3e illustrates a potential future style of deformation.

### 4. Interpretation of Model Results

In order to aid visual comparison with the strain map of central Afar (Figure 2), we rotate the model results by  $\sim 40^\circ$  to the left. Our reference model (Figures 3b–3e) uses an  $x$ -offset of 100 km and a lithospheric thickness of 70 km (Lavayssiere et al., 2018), which are similar to the observed scale of offset and lithospheric thickness in nature. This model reproduces key aspects of strain rate pattern seen in InSAR and GPS (Figures 2a–2c).

For the first 1 Myr, the rift segments extend without significant propagation along strike. After  $\sim 1$  Myr, deformation starts to localize at the rift segments and simultaneously the tips propagate to form an overlap zone (Figure 3b). Crustal blocks within the overlap rotate in a clockwise direction to accommodate the deformation field. After 2 Myr, diffuse deformation focuses onto a narrower ( $<50$  km wide) deformation zone and the tips merge by abandoning those faults bounding the overlap zone (Figure 3b). At 3 Myr (Figure 3c), the size of the overlap significantly decreases and deformation progressively localizes between the two rift segments. With further extension, at 4 Myr, a belt of overlapping, left-steeping, en-echelon zones form between the segments (Figure 3d). These segments resemble segmented continental rift basins that evolve into segmented oceanic rifts (Hayward & Ebinger, 1996). Ultimately, at 5 Myr (Figure 3e), the en-echelon segments merge to form a narrow, high strain rate zone that eventually links the two rift segments (Movie S1).

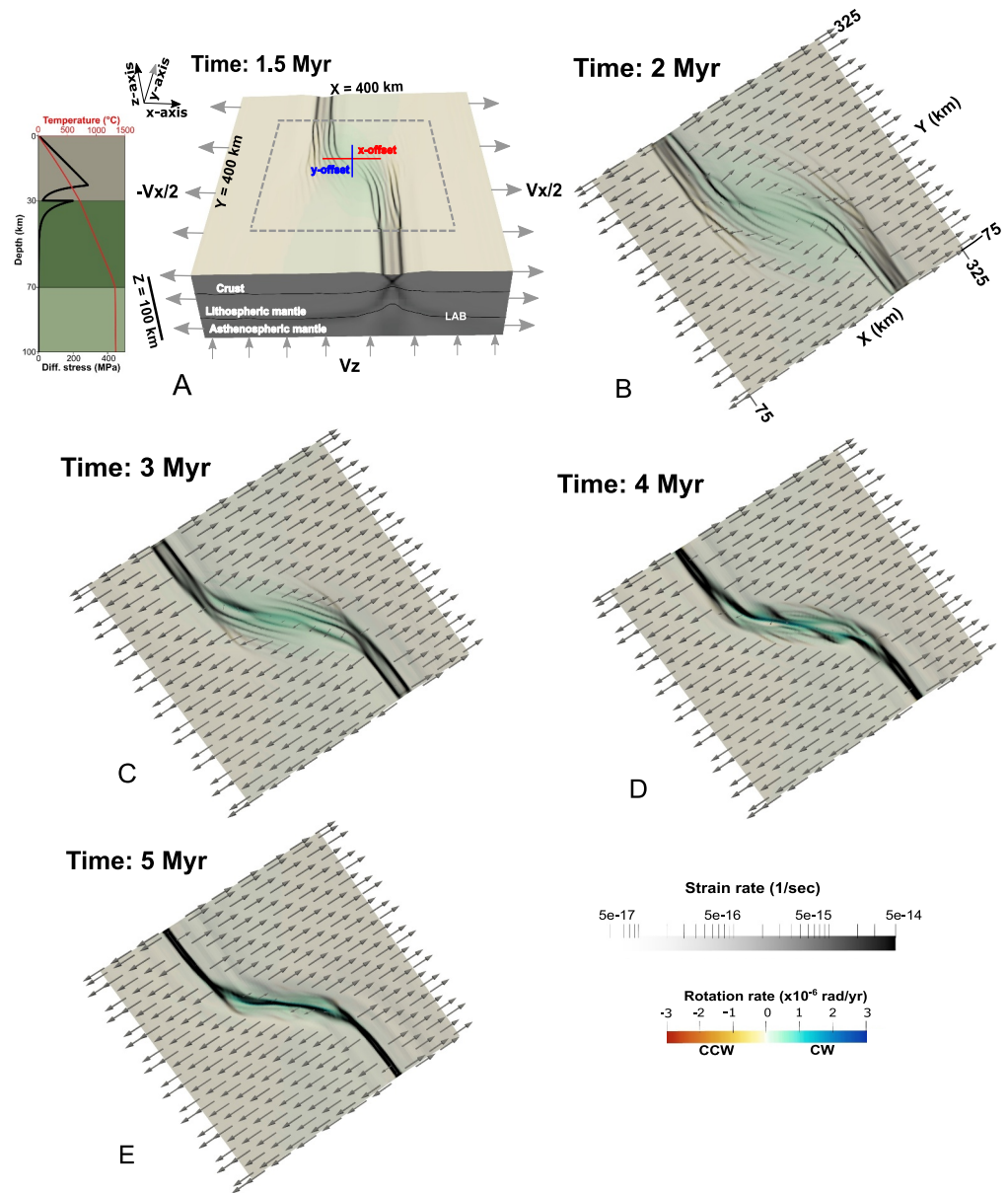


**Figure 3.** (a) 3D model setup forwarded to 1.5 Myr and yield strength envelope. The two parallel rift zones represent the Dabbahu-Manda Harraro and ASAL segments shown by thick white lines in Figure 1a.  $V_x$  and  $V_z$  represent the velocities in  $x$ - and  $z$ -directions. LAB—Lithosphere-Asthenosphere Boundary. The open gray box indicates the model domain presented in b–e. (b–e) Show snapshots of space-time evolution of rift linkage for  $x$ -offset of 100 km and lithospheric thickness of 70 km by tracking the instantaneous deformation rate. The time steps refer to the time since model initiation. Rotation rate is derived from horizontal velocity field. We interpret the rotation rate about a vertical axis where the velocity vectors indicate a clear rotational motion. Higher rotation rates can occur when the angle between the velocity vectors is high, which is not related to block-like motion. CCW- Counterclockwise; CW- Clockwise. Refer to the Supporting Information S1 documents for model animation.

Our test of the tectonic regimes at 3 Myr (Figures 4a–4i; Movies S2–S9) allows us to detect possible styles of rift connections for a combination of lithospheric thicknesses and  $x$ -offsets. An  $x$ -offset of 50 km allows for a direct linkage to form via a curved rift irrespective of the lithospheric thickness variation (Figures 4a, 4d, and 4g). A larger  $x$ -offset (150 km; Figures 4c, 4f and 4i) prohibits direct linkage between rift segments and leads to the formation of a micro-block that homogeneously rotates about a vertical axis (Duclaux et al., 2020; Neuharth et al., 2021). Drastic changes in tectonic regime from block rotation to linkage by a curved rift zone occurs for an  $x$ -offset of 100 km and lithospheric thickness varying from 60 to 80 km (Figures 4b, 4e, and 4h). We suggest that

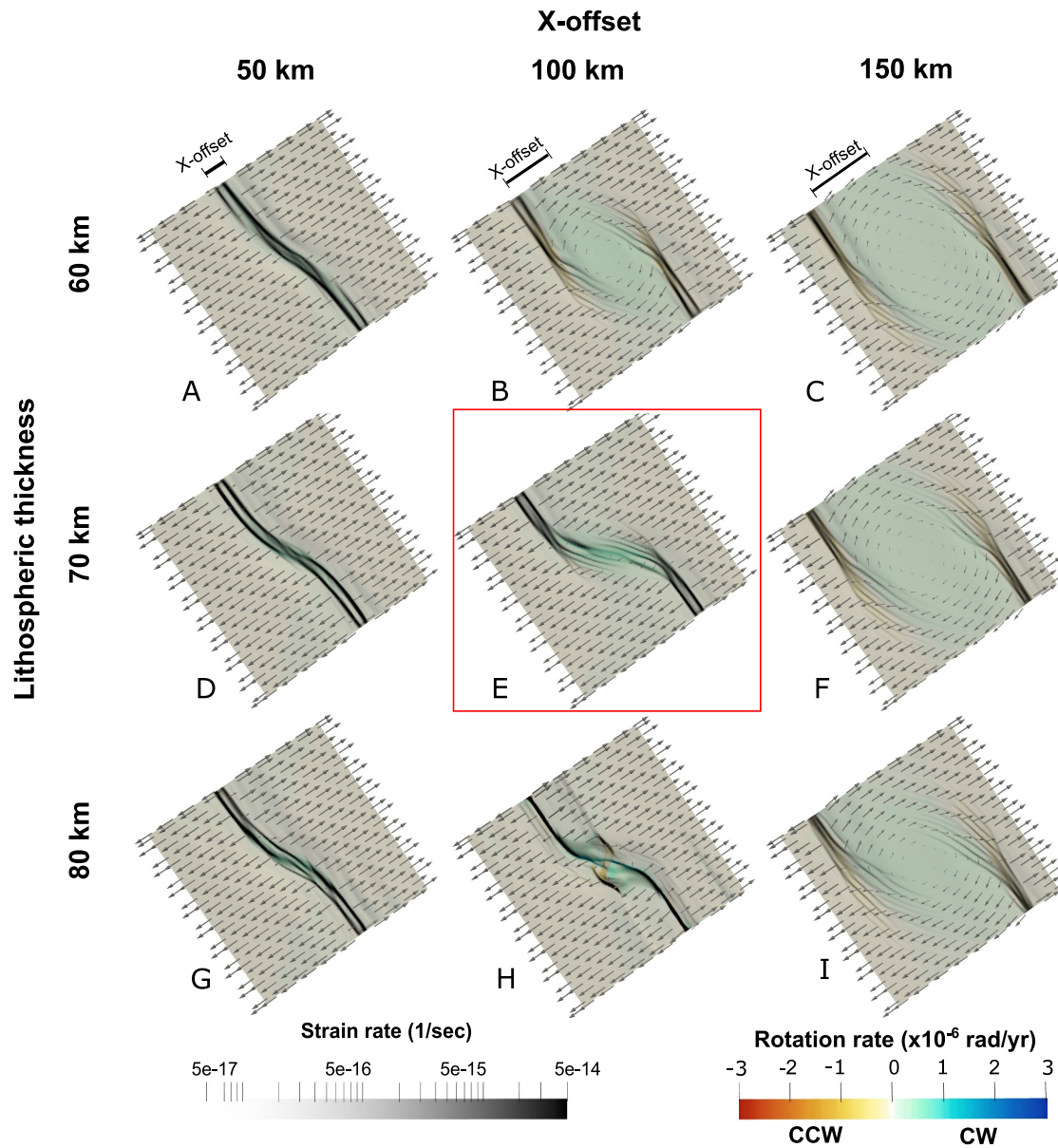


**Figure 4.** Regime diagram at 3 Myr for ranges of x-offset and lithospheric thickness. The tectonic regime remains the same irrespective of the lithospheric thickness for x-offsets of 50 and 150 km. For x-offset of 100 km, the tectonic regime changes from block rotation to linkage via curved rift as the lithospheric thickness increases. The red rectangle indicates the reference model shown in Figure 3. Refer to the Supporting Information S1 documents for model animations.

thicker lithosphere and therefore colder enhances plastic strain localization and favors direct linkage (Figure 4h). On the other hand, thinner lithosphere encourages diffuse deformation generating overlapping rifts (Figure 4b). A similar style of tectonic regime change (i.e., overlap to direct linkage) is observed in Neuharth et al. (2021) when models are conducted for a stronger lithosphere. In order to test the robustness of our model, we conduct additional experiment using granulite (Wilks & Carter, 1990) flow law for the crust. With the exception of delayed strain localization, the pattern of rift connection remains consistent with our reference model.

### 5. Connection Between the Red Sea and Gulf of Aden Rifts

Competing models for the connection between the RS and the GoA rifts suggest that the two rifts either directly link or form an overlap zone. The overlap scenario bases its argument on paleomagnetic observations from ~1–2 Myr old volcanic units in central Afar; accordingly, crustal blocks within the overlap rotate in a clockwise sense

(Acton et al., 1991; Kidane et al., 2003). Although the paleomagnetic studies suggest a similar sense of rotation, the detailed mechanisms to explain the rotation are different. For example, Kidane et al. (2003) proposed that the overlap is accommodated by rift parallel, sinistral strike slip faults that are arranged in a “bookshelf” manner (Tapponnier et al., 1990), whereas the model by Acton et al. (1991) argues that rotation of the blocks within the overlap is a kinematic consequence of strain transfer between the growing and dying rifts at their tips. Combining our model result at 2 Myr (Figure 3b) with earthquake focal mechanisms in the region (Figure 2; Craig et al., 2011), we suggest that block rotation in central Afar occurred without bookshelf faulting.

The present-day deformation rates derived from InSAR and GPS (Figures 2a–2c) show not only focused deformation at the DMH and ASAL segments but also a zone of high strain rate that occurs in the linkage zone between the two segments (Figure 2c). A number of recent geophysical and geological observations corroborate this argument. For example, slip rate analysis from the Dobi graben (Figure 1a) shows that faults exhibit increasing slip rates both to the NW- and SE-directions from the graben, which eventually transfer the strain between the DMH and ASAL segments (Demissie et al., 2023). Earthquake swarm analysis from the Afar rift suggests that the Dobi and Serdo basins are the loci of incipient deformation in central Afar (Ruch et al., 2021). Similarly, detailed earthquake catalog analysis shows an ~ E–W oriented pattern of seismicity between the segments induced by dextral shearing (Pagli et al., 2018). The above-mentioned deformation patterns are best reflected by our reference model at 3–4 Myr (Figure 3). In summary, slip-rate analysis, and earthquake swarm studies confirm that the linkage between the RS and GoA rifts is accommodated by a transtensional deformation zone that eventually paves the way for a direct linkage via a proto-transform fault.

Previous numerical models observed a similarly complex and time-dependent evolution of connection between propagating rifts. For example, Illsley-Kemp et al. (2018) demonstrated that strain localization at the tips of propagating rifts in Northern Afar can induce proto-transform fault linkage. This study however does not explain the connection through block rotation observed in central Afar. The oblique rifting model by Duclaux et al. (2020) provided insights on direct linkage of segments prior to break-up, but did not encompass a phase of initial block rotation. Our work reproduces the observed spatiotemporal evolution of the linkage system in central Afar. Importantly, we demonstrate that rift linkage is highly dynamic and can involve significant changes in rotation and fault kinematics through space and time.

## 6. Conclusions

A detailed understanding on how the connection between propagating rifts occurs is crucial to capture the dynamics of continental break-up and the onset of seafloor spreading. The mechanism of linkage between the RS and GoA rifts in central Afar has long been debated. We use high resolution InSAR and geodynamic modeling to understand the evolution of linkage between the RS and GoA rifts during the last ~4 million years. We demonstrate that the connection between the two rifts is best explained by progressive localization of deformation from overlapping segments to direct linkage involving en-echelon basins and proto-transform fault. These results reconcile contrasting views and conclusively demonstrate that the connection between rifts is a dynamic process that involves significant changes in style over time and space.

## Data Availability Statement

The earthquake data plotted in Figures 1 and 2 can be found in Pagli et al. (2018). We use ASPECT (version 2.4.0), which is open source and can be downloaded at <https://aspect.geodynamics.org/>. The input files and source code are available here: <https://zenodo.org/doi/10.5281/zenodo.11619586>.

## References

- Acton, G., Stein, S., & Engeln, J. (1991). Block rotation and continental extension: A microplate model for Afar. *Tectonics*, *10*(3), 501–526. <https://doi.org/10.1029/90tc01792>
- Ahmed, A., Doubré, C., Leroy, S., Keir, D., Pagli, C., Hammond, J. O., et al. (2022). Across and along-strike crustal structure variations of the western Afar margin and adjacent plateau: Insights from receiver functions analysis. *Journal of African Earth Sciences*, *192*, 104570. <https://doi.org/10.1016/j.jafrearsci.2022.104570>
- Allken, V., Huismans, R. S., & Thieulot, C. (2012). Factors controlling the mode of rift interaction in brittle-ductile coupled systems: A 3D numerical study. *Geochemistry, Geophysics, Geosystems*, *13*(5). <https://doi.org/10.1029/2012GC004077>
- Almalki, A., & Betts, P. (2021). Gulf of Aden spreading does not conform to triple junction formation. *Geology*, *49*(6), 672–676. <https://doi.org/10.1130/G48529.1>

## Acknowledgments

AM acknowledges support from Alexander von Humboldt foundation. The development of ASPECT is funded by the National Science Foundation under award EAR-0949446 and EAR-1550901 to the Computational Infrastructure for Geodynamics ([www.geodynamics.org](http://www.geodynamics.org)). SB has been funded by the European Union (ERC, EMERGE, 101087245). CP, ALR, DK, GC were supported by Ministero dell'Università e della Ricerca (MiUR) through PRIN Grant 2017P9AT72. We gratefully acknowledge the computing time granted by the Resource Allocation Board and provided on the supercomputer Lise and Emmy at NHR@ZIB and NHR@Göttingen as part of the NHR infrastructure. The calculations for this research were conducted with computing resources under the project bfp00064. We used the scientific color maps from Cramer et al. (2020) to draft the figures using Generic Mapping tools, Paraview and Inkscape. We thank the anonymous reviewers for constructive and critical comments and the editor, Fabio Capitanio, for editorial handling of our manuscript.



- Balázs, A., Gerya, T., May, D., & Tari, G. (2023). *Contrasting transform and passive margin subsidence history and heat flow evolution: Insights from 3D thermo-mechanical modelling*. Geological Society, London, Special Publications. <https://doi.org/10.1144/sp524-2021-94>
- Bastow, I., Nyblade, A., Stuart, G., Rooney, T., & Beniot, M. H. (2008). Upper mantle seismic structure beneath the Ethiopian hot spot: Rifting at the edge of the African low-velocity anomaly. *Geochemistry, Geophysics, Geosystems*, 9(12). <https://doi.org/10.1029/2008GC002107>
- Brune, S., Corti, G., & Ranalli, G. (2017). Controls of inherited lithospheric heterogeneity on rift linkage: Numerical and analog models of interaction between the Kenyan and Ethiopian rifts across the Turkana depression. *Tectonics*, 36(9), 1767–1786. <https://doi.org/10.1002/2017TC004739>
- Cardozo, N., & Allmendinger, R. (2009). SSPX: A program to compute strain from displacement/velocity data. *Computers and Geology*, 35(6), 1343–1357. <https://doi.org/10.1016/j.cageo.2008.05.008>
- Chambers, E., Haromn, N., Rychert, C., Gallacher, R., & Keir, D. (2022). Imaging the seismic velocity structure of the crust and upper mantle in the northern East African rift using Rayleigh wave tomography. *Geophysical Journal International*, 230(3), 2036–2055. <https://doi.org/10.1093/gji/ggac156>
- Craig, T., Jackson, A., Priestley, K., & McKenzie, D. (2011). Earthquake distribution patterns in Africa: Their relationship to variations in lithospheric and geological structure, and their rheological implications. *Geophysical Journal International*, 185(1), 403–434. <https://doi.org/10.1111/j.1365-246x.2011.04950.x>
- Cramer, F., Shephard, G., & Heron, P. (2020). The misuse of colour in science communication. *Nature Communications*, 11(1), 5444. <https://doi.org/10.1038/s41467-020-19160-7>
- Demissie, Z., Bedassa, G., Rattani, A., Nigussie, W., Kebede, H., Muhabaw, Y., & Haridasan, S. (2023). The significance of volcanic segments and rifts in faults characterization within the a magmatic graben of the afar depression, Ethiopia. *Journal of Structural Geology*, 174, 104914. <https://doi.org/10.1016/j.jsg.2023.104914>
- Dobre, C., Deprez, A., Masson, F., Socquet, A., Lewi, E., Grandin, R., et al. (2017). Current deformation in central afar and triple junction kinematics deduced from GPS and InSAR measurements. *Geophysical Journal International*, 208(2), 936–953. <https://doi.org/10.1093/gji/ggw434>
- Drouin, V., Sigmundsson, F., Ofeigsson, G., Herinsdottir, S., Strukell, E., & Einarsson, P. (2017). Deformation in the northern volcanic zone of Iceland 2008–2014: An interplay of tectonic, magmatic, and glacial isostatic deformation. *Journal of Geophysical Research: Solid Earth*, 122(4), 3158–3178. <https://doi.org/10.1002/2016jb013206>
- Duclaux, G., Huismans, R., & May, D. (2020). Rotation, narrowing, and preferential reactivation of brittle structures during oblique rifting. *Earth and Planetary Science Letters*, 531, 115952. <https://doi.org/10.1016/j.epsl.2019.115952>
- Dugda, M., Nyblade, A., Julia, J., Langston, C., Ammon, C., & Simiyu, S. (2005). Crustal structure in Ethiopia and Kenya from receiver function analysis: Implications for rift development in eastern Africa. *Journal of Geophysical Research*, 110(B1). <https://doi.org/10.1029/2004jb003065>
- Ebinger, C., Yemane, T., Harding, D., Tesfaye, S., Kelley, S., & Rex, D. (2000). Rift deflection, migration, and propagation: Linkage of the Ethiopian and eastern rifts: Africa. *GSA Bulletin*, 112(2), 163–176. [https://doi.org/10.1130/0016-7606\(2000\)112<0163:rdmapl>2.3.co;2](https://doi.org/10.1130/0016-7606(2000)112<0163:rdmapl>2.3.co;2)
- Ferguson, D., MacLennan, J., Bastow, I., Pyle, D., Jones, S., Keir, D., et al. (2013). Melting during late-stage rifting in afar is hot and deep. *Nature*, 499(7456), 70–73. <https://doi.org/10.1038/nature12292>
- Gassmüller, R., Lokavarpu, H., Heien, E., Puckett, E., & Bangerth, W. (2018). Flexible and scalable particle-in-cell methods with adaptive mesh refinement for geodynamic computations. *Geochemistry, Geophysics, Geosystems*, 19(9), 3596–3604. <https://doi.org/10.1029/2018gc007508>
- Glerum, A., Brune, S., Stamps, D., & Strecker, M. (2020). Victoria continental microplate dynamics controlled by the lithospheric strength distribution of the East African rift. *Nature Communications*, 11(1), 2881. <https://doi.org/10.1038/s41467-020-16176-x>
- Glerum, A., Thieulot, C., Fraters, M., Blom, C., & Spakman, W. (2018). Nonlinear viscoelasticity in ASPECT: Benchmarking and applications to subduction. *Solid Earth*, 9(2), 267–294. <https://doi.org/10.5194/se-9-267-2018>
- Hammond, J., Kendall, M., Stuart, G., Keir, D., Ebinger, C., Ayele, A., & Belachew, M. (2011). The nature of the crust beneath the afar triple junction: Evidence from receiver functions. *Geochemistry, Geophysics, Geosystems*, 12. <https://doi.org/10.1029/2011GC003738>
- Hayward, N., & Ebinger, C. (1996). Variations in along-axis segmentation of the afar rift system. *Tectonics*, 15(2), 244–257. <https://doi.org/10.1029/95tc02292>
- Heister, T., Dannberg, J., Gassmüller, R., & Bangerth, W. (2017). High accuracy mantle simulation through modern numerical methods-ii: Realistic models and problems. *Geophysical Journal International*, 210(2), 833–851. <https://doi.org/10.1093/gji/ggx195>
- Hirth, G., & Kohlstedt, D. (2003). *Rheology of the upper mantle and the mantle wedge: A view from the experimentalists: Inside the subduction factory* (Vol. 183). Geophysical Monograph.
- Illsley-Kemp, F., Bull, J., Keir, D., Gerya, T., Pagli, C., Gernon, T., et al. (2018). Initiation of a proto-transform fault prior to seafloor spreading. *Geochemistry, Geophysics, Geosystems*, 19(12), 4744–4756. <https://doi.org/10.1029/2018GC007947>
- Kidane, T., Courtillot, V., Manighetti, I., Audin, L., Lahitte, P., Quidelleur, X., et al. (2003). New paleomagnetic and geochronologic results from Ethiopian Afar: Block rotations linked to rift overlap and propagation and determination of a 2 Ma reference pole for stable Africa. *Journal of Geophysical Research*, 108(B2). <https://doi.org/10.1029/2001JB000645>
- Kolawole, F., Firkins, M., Wahaibi, T. A., Atekwana, E., & Soreghan, M. (2021). Rift interaction zones and the stages of rift linkage in active segmented continental rift systems. *Basin Research*, 33(6), 2984–3020. <https://doi.org/10.1111/bre.12592>
- Kronbichler, M., Heister, T., & Bangerth, W. (2012). High accuracy mantle convection simulation through modern numerical methods. *Geophysical Journal International*, 191(1), 12–29. <https://doi.org/10.1111/j.1365-246x.2012.05609.x>
- La Rosa, A., Pagli, C., Hurman, G., & Keir, D. (2022). Strain accommodation by intrusion and faulting in a rift linkage zone: Evidences from high resolution topography data of the Afrera plain (afar, East Africa). *Tectonics*, 41(6). <https://doi.org/10.1029/2021TC007115>
- Lavaysiere, A., Rycher, C., Hermon, N., Keir, D., Hammond, J., Kendall, M., et al. (2018). Imaging lithospheric discontinuities beneath the northern East African rift using s-to-p receiver functions. *Geochemistry, Geophysics, Geosystems*, 10. <https://doi.org/10.1029/2018GC007463>
- Le Pourhiet, L., May, D., Huille, L., Watremez, L., & Leroy, S. (2017). A genetic link between transform and hyper-extended margins. *Earth and Planetary Science Letters*, 465, 184–192. <https://doi.org/10.1016/j.epsl.2017.02.043>
- Maestrelli, D., Brune, S., Corti, G., Keir, D., Muluneh, A., & Sani, F. (2022). Analogue and numerical modeling of rift-rift-rift triple junctions. *Tectonics*, 41(10). <https://doi.org/10.1029/2022TC007491>
- Manighetti, I., Tapponnier, P., Gillot, P., Jacques, E., Courtillot, V., Armijo, J., et al. (1998). Propagation of rifting along the Arabia-Somalia plate boundary: Into afar. *Journal of Geophysical Research*, 103(B3), 4947–4974. <https://doi.org/10.1029/97jb02758>
- McClusky, S., Reilinger, R., Ogubazghi, G., Amleson, A., Healeb, B., Vernant, P., et al. (2010). Kinematics of the southern red sea-afar triple junction and implications for plate dynamics. *Geophysical Research Letters*, 37(5). <https://doi.org/10.1029/2009GL011127>
- Moore, C., Wright, T., & Hooper, A. (2021). Rift focusing and magmatism during late-stage rifting in afar. *Journal of Geophysical Research*, 126(10). <https://doi.org/10.1029/2020JB21542>



- Muluneh, A., Kidane, T., Rowland, J., & Bachtadse, V. (2013). Counterclockwise block rotation linked to southward propagation and overlap of sub-aerial red sea rift segments, afar depression: Insight from paleomagnetism. *Tectonophysics*, 593, 111–120. <https://doi.org/10.1016/j.tecto.2013.02.030>
- Nelson, R., Patton, T., & Morley, C. (1992). Rift-segment interaction and its relation to hydrocarbon exploration in continental rift systems. *AAPG Bulletin*, 76, 1153–1169. <https://doi.org/10.1306/bdff898e-1718-11d7-8645000102c1865d>
- Neuharth, D., Brune, S., Glerum, A., Heine, C., & Welford, K. (2021). Formation of continental microplates through rift linkage: Numerical modeling and its application to the Flemish Cap and Sao Paulo plateau. *Geochemistry, Geophysics, Geosystems*, 22(4). <https://doi.org/10.1029/2020GC009615>
- Pagli, C., Wang, H., Wright, T., Calais, E., & Lewi, E. (2014). Current plate boundary deformation of the afar rift from a 3D velocity field inversion of InSAR and GPS. *Journal of Geophysical Research*, 119(11), 8562–8575. <https://doi.org/10.1002/2014jb011391>
- Pagli, C., Yun, S., Ebinger, C., Keir, D., & Wang, H. (2018). Strike-slip tectonics during rift linkage. *Geology*, 47(1), 31–34. <https://doi.org/10.1130/G45345.1>
- Polun, S., Gomez, F., & Tesfaye, S. (2018). Scaling properties of normal faults in the central afar, Ethiopia and Djibouti: Implications for strain partitioning during the final stages of continental breakup. *Journal of Structural Geology*, 115, 178–189. <https://doi.org/10.1016/j.jsg.2018.07.018>
- Rime, V., Foubert, A., Ruch, J., & Kidane, T. (2023). Tectonostratigraphic evolution and significance of the afar depression. *Earth-Science Reviews*, 244, 104519. <https://doi.org/10.1016/j.earscirev.2023.104519>
- Rose, L., Buffett, B., & Heister, T. (2017). Stability and accuracy of free surface time integration in viscous flows. *Physics of the Earth and Planetary Interiors*, 262, 90–100. <https://doi.org/10.1016/j.pepi.2016.11.007>
- Ruch, J., Keir, D., Passarelli, L., Giacomo, D. D., Ogubazghi, G., & Jonsson, S. (2021). Reveling 60 years of earthquake swarms in the southern red sea, Afar and the Gulf of Aden. *Frontiers in Earth Science*, 9. <https://doi.org/10.3389/feart.2021.664673>
- Rybacki, E., Gottschalk, M., Wirth, R., & Dresen, G. (2006). Influence of water fugacity and activation volume on the flow properties of fine-grained anorthite aggregates. *Journal of Geophysical Research*, 111(3). <https://doi.org/10.1029/2005/JB003663>
- Tapponnier, P., Armijo, R., Manighetti, I., & Courtillot, V. (1990). Bookshelf faulting and horizontal block rotations between overlapping rifts in southern afar. *Geophysical Research Letters*, 17, 1–4. <https://doi.org/10.1029/gl017i001p00001>
- Vigny, C., de Chabaliere, J., Ruegg, J., Huchon, P., Feigl, K., Cattin, R., et al. (2007). Twenty five years of geodetic measurements along the Tadjoura-Asal rift system, Djibouti, East Africa. *Journal of Geophysical Research*, 112(B6). <https://doi.org/10.1029/2004JB003230>
- Wang, M., & Shen, Z.-K. (2020). Present-day crustal deformation of continental China derived from GPS and its tectonic implications. *Journal of Geophysical Research*, 125(2). <https://doi.org/10.1029/2019JB018774>
- Wang, T., Gao, S., Yang, Q., & Liu, K. (2021). Crustal structure beneath the Ethiopian plateau and adjacent areas from receiver functions: Implications for partial melting and magmatic underplating. *Tectonophysics*, 809, 228857. <https://doi.org/10.1016/j.tecto.2021.228857>
- Watts, E., Gernon, T., Taylor, R., Keir, D., & Pagli, C. (2023). Magmatic evolution during proto-oceanic rifting at Alu, Dalafilla and Borale volcanoes (afar) determined by trace element and Sr-Nd-Pb isotope geochemistry. *Lithos*, 456–457, 456–457. <https://doi.org/10.1016/j.lithos.2023.107311>
- Wilks, K., & Carter, N. (1990). Rheology of some continental lower crustal rocks. *Tectonophysics*, 182(1–2), 57–77. [https://doi.org/10.1016/0040-1951\(90\)90342-6](https://doi.org/10.1016/0040-1951(90)90342-6)
- Wolf, L., Huisman, R., Wolf, S., Rouby, G., & May, D. (2022). Evolution of rift architecture and fault linkage during continental rifting: Investigating the effects of tectonics and surface processes using lithospheric-scale 3D coupled numerical models. *Journal of Geophysical Research*, 127(12). <https://doi.org/10.1029/2022JB024687>
- Wolfenden, E., Ebinger, C., Yirgu, G., Deino, A., & Ayalew, D. (2004). Evolution of the northern main Ethiopian rift: Birth of a triple junction. *Earth and Planetary Science Letters*, 224(1–2), 213–228. <https://doi.org/10.1016/j.epsl.2004.04.022>
- Wright, T., Ebinger, C., Biggs, J., Ayele, A., Yirgu, G., Keir, D., & Stock, A. (2006). Magma-maintained rift segmentation at continental rupture in the 2005 afar dyking episode. *Nature*, 442(100), 291–294. <https://doi.org/10.1038/nature04978>
- Zwaan, F., & Schreurs, G. (2017). How oblique extension and structural inheritance influence rift segment interaction: Insights from 4D analog models. *Interpretation*, 5(1), 119–138. <https://doi.org/10.1190/int-2016-0063.1>